FULL PAPER

Combined volcano-tectonic processes for the drowning of the Roman western coastal settlements at Campi Flegrei (southern Italy)

Stefano Vitale* and Jacopo Natale

Abstract

The active Campi Flegrei caldera in southern Italy has a remarkably long history of coexistence between volcanism and human settlements, and it is famous for its peculiar slow ground movement called bradyseism, i.e. episodes of inflation and deflation of the caldera floor due to magmatic and/or hydrothermal processes. This natural phenomenon has interacted with the civilization that inhabited this strategic and fertile area, especially in Roman times, when the sinking of the coast hindered the flourishment of *Puteoli* and *Baiae* coastal towns. The drowning of a large part of Republic-early Imperial Roman coastal buildings, west of the modern Pozzuoli town, is classically used to illustrate the bradyseism activity. In this paper, we investigate the spatial variability and the role of this phenomenon, demonstrating that the caldera deflation alone cannot account for the submersion of Roman facilities in the western sector where the harbour structures of *Portus Iulius* and luxury villas of the *Baianus Lacus* presently lie beneath sea level. On the contrary, the sinking of this area is mainly the result of the activity of volcano-tectonic faults. We restored the topography to 100 BCE using archaeological and high-resolution topographic data. Results show that the several metres of vertical displacement recorded in the Baia area in the last 2100 yr were mainly produced by the activity of normal faults and secondarily by caldera deflation, the former including the long-lived Baia Fault and the younger normal faults associated with the Monte Nuovo eruption at 1538 CE.

Keywords Campi Flegrei, Bradyseism, Caldera deformation, Volcano-tectonics, Faults, Archeological markers

Graphical Abstract
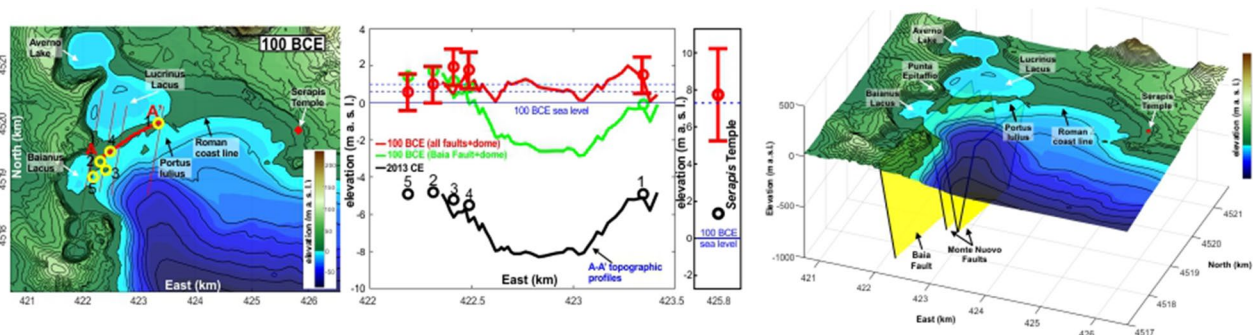
*Correspondence:
Stefano Vitale
stefano.vitale@unina.it
Full list of author information is available at the end of the article

Introduction

People have inhabited the area of Campi Flegrei (Fig. 1a; southern Italy) since 10 ka, and lastingly since the Eneolithic (e.g., Costa et al. 2022). Due to the strategic position, fertile soils, and accessible resources, Greeks first and Romans then built along the coast different towns, including *Cumae* (Cuma), *Puteoli* (Pozzuoli), *Misenum* (Miseno), *Bauli* (Bacoli), and *Baiae* (Baia; Fig. 1a). In this context, the life of Romans has dealt with the complex volcano-tectonic activity that characterized the history of the Campi Flegrei from the Late Imperial period on, when part of the western sector of the caldera was gradually submerged. In fact, in the last 2100 yr, the central sector of the caldera experienced alternating phases of ground subsidence and uplift with maximum values centred in the Pozzuoli area. This phenomenon, associated with magmatic and/or hydrothermal processes, is locally indicated by the historical term of bradyseism (e.g., Parascandola 1947; Orsi et al. 2022). Geological and archaeological studies carried out in the last decades allowed the reconstruction of the vertical ground displacement from Roman times (Bellucci et al. 2006; Del Gaudio et al. 2010; Dvorak and Mastrolorenzo 1991; Morhange et al. 1999, 2006; Di Vito et al. 2016; Fig. 1b) for the central caldera sector (*Serapis* Temple; Fig. 1a). These studies indicate that ground uplift and subsidence have alternated through time (Fig. 1b), with maximum values of uplift and subsidence in the range of metres, centred close to the Pozzuoli town, also preceding and following, respectively, the 1538 CE Monte Nuovo eruption

(Di Vito et al. 2016), resembling the same pattern of the long-term (~ 10 ka) deformation (Natale et al. 2022a, b), and of recent unrests (Bevilacqua et al. 2020; Isaia et al. 2019). Recently, the caldera experienced four major uplift episodes (Fig. 1c). The main uplift occurred in 1982–1984 (Berrino et al. 1984; De Siena et al. 2017). In contrast, the ongoing unrest started in 2005 with a vertical displacement rate one order of magnitude smaller than previous unrest episodes (Fig. 1c). The maximum uplift was reached in 1984 with 3.82 m compared to the 1950 baseline (Del Gaudio et al. 2010), recorded at levelling benchmark 25A in the centre of Pozzuoli town (Fig. 1a). Such unrest episodes may represent the short-term inflation events that incrementally produce the long-term caldera resurgence (e.g., Acocella 2019).

In the following analysis and discussion, we consider the bradyseism phenomenon as the alternating ground uplift and subsidence phases defined by an axis-symmetric bell-shaped pattern accordingly to the historical reconstructions (e.g., Di Vito et al. 2016) and the recent recordings (e.g., Amoruso et al. 2014; Berrino et al. 1984; Bevilacqua et al. 2020; De Siena et al. 2017; Del Gaudio et al. 2010; Dvorak and Mastrolorenzo 1991).

A scientific debate still exists on the origin of such inflation/deflation deformation, whether it is related to the magma intrusion, pressurization/depressurization of the hydrothermal system, or a combination of both (Amoruso et al. 2014; Battaglia et al. 2006; D'Auria et al. 2015; De Natale et al. 2006; Lima et al. 2009; Macedonio et al. 2014; Todesco et al. 2006, 2014; Woo and Kilburn
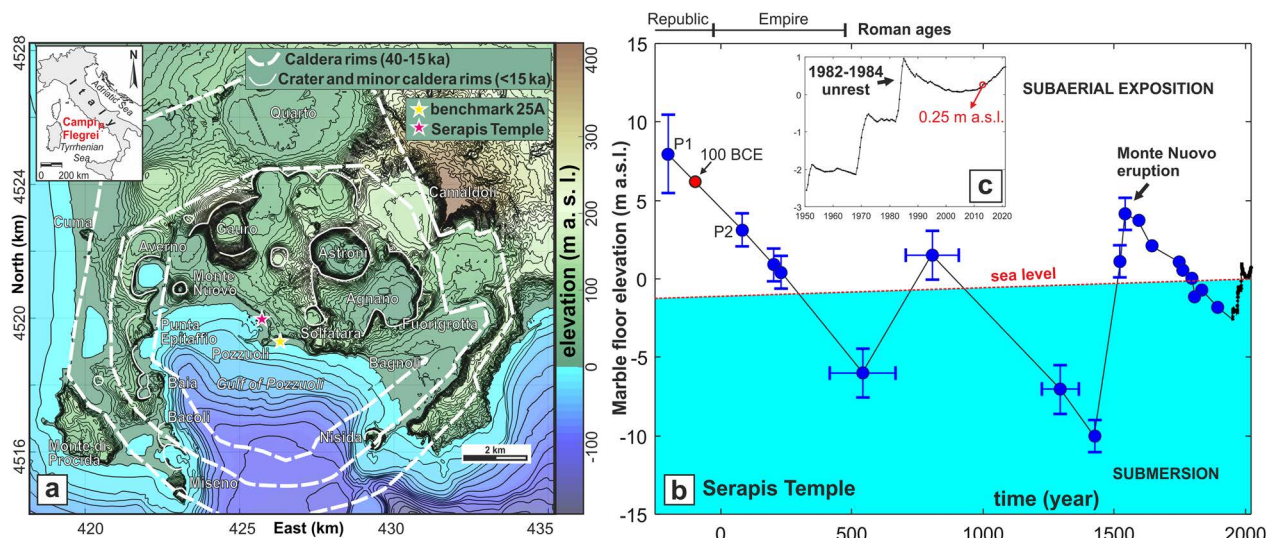
Fig. 1 a DEM of the Campi Flegrei caldera showing the main crater and caldera rims. **b** Vertical displacement of the *Serapis* Temple marble floor in the last 2200 yr (data from Morhange et al. 1999; Bellucci et al. 2006). The sea-level change curve of the Campania sector is also shown (data from Lambeck et al. 2011). **c** Vertical displacement of the *Serapis* Temple marble floor (Pozzuoli) compared to the 1950 baseline until 2021 (modified after Del Gaudio et al. 2010)

2010). However, the discussion about the source of the inflation/deflation deformation is beyond the scope of this paper. At the same time, we focus on the competing contribution to the deformation pattern between caldera inflation/deflation processes and volcano-tectonic faulting.

The rich heritage of Roman ruins and their relationships with the geological history of the Campi Flegrei has attracted scholars' interest since the nineteenth century (Lyell 1830–1833). The *Serapis* Temple (*Macellum*, Roman market, Fig. 2a) soon became the symbol of bradyseism, and the *Lithophaga* mollusc burrows, together with other archaeological features, were used as vertical markers for the reconstruction of ground movements (Lyell 1830–1833; Bellucci et al. 2006; Morhange et al. 1999, 2006; Parascandola 1947; Aucelli et al. 2020; Marino et al. 2022). Because of ground subsidence, a large part of the former Roman coast is presently underwater (Fig. 2b-d), including the harbour (*Portus Iulius*; Fig. 2b), the villas (Fig. 2c), and the *Baianus Lacus* area (Fig. 2d, e). Since 37 BCE, the former *Lucrinus Lacus* was connected with the Averno Lake by a narrow channel

and hosted the harbour structures of the *Portus Iulius* (Aucelli et al. 2020; Fig. 2e). This port was first built as a military facility and then converted for commercial purposes in the first century BCE, with the Roman fleet (*Classis Misenensis*) later transferred to the nearby Miseno harbour (Aucelli et al. 2020). The *Portus Iulius* (Fig. 2e) was protected from the sea-storm waves by a long coastal sand spit, on which, at the end of the late Republic age, Romans built the road Via *Herculanea*, connecting Punta Epitaffio to *Puteoli* (Fig. 2e), subsequently reinforced by a series of *pilae*, cubic concrete blocks made up of a mixture of *pozzolana* (ash) and lime (e.g., Rispoli et al. 2020), that served as a breakwater. The shore along the *Baianus Lacus* was a residential area that featured thermal facilities and luxury villas, including *Villa dei Pisoni* and the *Villa a Protiro* (Fig. 2c, d). The morphological high of *Secca Delle Fumose* (Smoking Shoals; Fig. 2d, e) is present between these two sectors and is currently characterized by hot gas emission (Di Napoli et al. 2016; Vaselli et al. 2011). This part of the coast was abandoned during the late Imperial Roman period (fourth century) due to the relentless subsidence
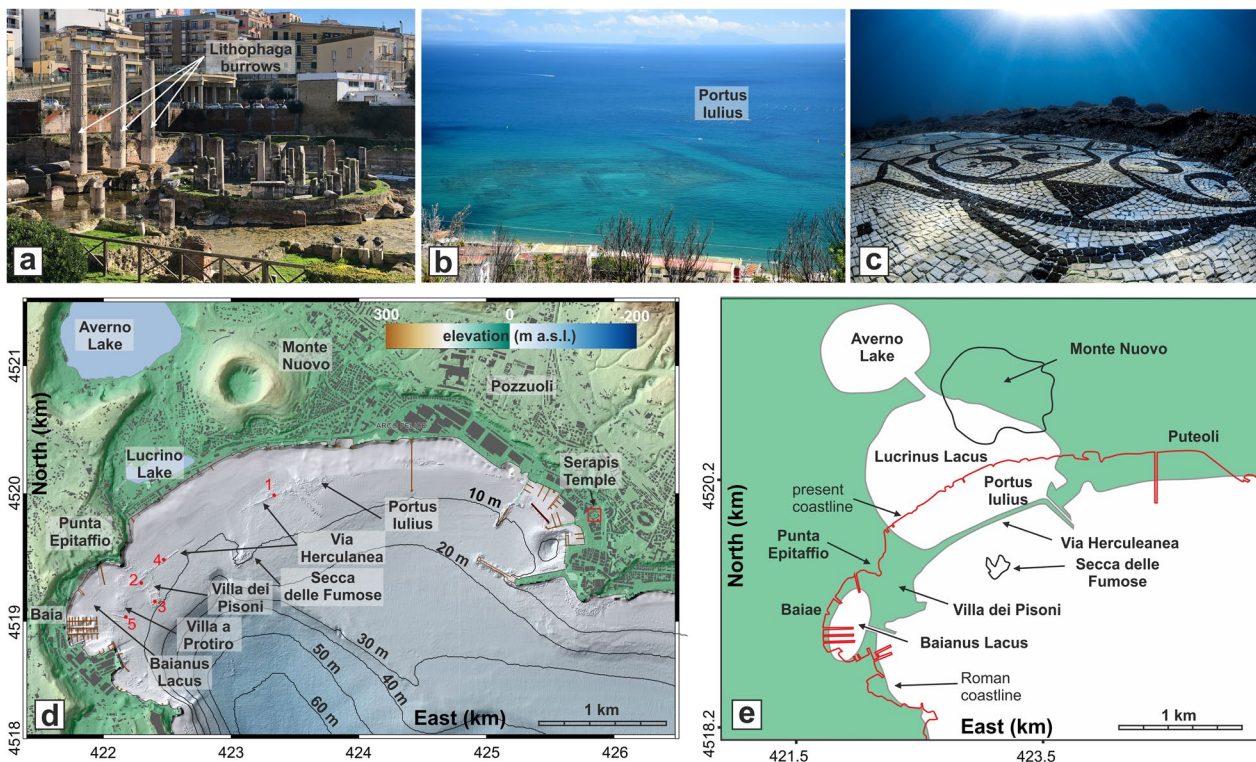

Fig. 2 **a** The *Serapis* Temple picture shows the *Lithophaga* mollusc burrows along the marble columns and the marble floor (photo by the authors). **b** Panoramic view of the submerged harbour structures of *Portus Iulius* as seen from Monte Nuovo (photo by the authors). **c** Submerged mosaic of *Villa a Protiro* (courtesy of Edoardo Ruspantini and Parco Archeologico dei Campi Flegrei). **d** The map shows the presently submerged *Portus Iulius* and *Baianus Lacus* areas (modified after Somma et al. 2016). Locations of archaeological data (red dots) used for the topographic restoration are also reported (data from Passaro et al. 2013). **e** Morphological reconstruction of the *Portus Iulius* and Roman coast (modified after Passaro et al. 2013; Di Vito et al. 1987; Ascione et al. 2020)

and subsequent marine ingression (Aucelli et al. 2020). Presently this area is submerged by as much as 5–8 m, constituting a marine protected reserve and an archaeological site (Parco Sommerso di Baia; http://www.parco sommersobaia.beniculturali.it/it). Several studies on the submerged Roman buildings highlighted the evidence of the marine ingression that changed the coastline, among others Passaro et al. (2013), using a DTM (Digital Terrain Model) with 0.1 m maximum grid resolution in the archaeological sites, estimated a mean subsidence rate of 2.9 mm/y for the western area of Pozzuoli Gulf. The Authors also emphasized that drowning was not equal for all sectors, but it shows significant variations from *Baianus Lacus* to *Portus Iulius*. Moreover, since Roman times the sea level has risen only as much as about 1 m along the Campania coast (Lambeck et al. 2011), unable to account for the submersion of such structures. Indeed, the submersion of Roman buildings is frequently used as an example of the effect of bradyseism (Aucelli et al. 2017; Costa et al. 2022; Passaro et al. 2013). Nonetheless, so far, no research has demonstrated this not trivial relationship. This study investigates the causes behind the drowning of the western coast of Campi Flegrei, trying to evaluate the contributions of two possibly combined processes: caldera inflation/deflation deformation and volcano-tectonic faulting.

The observations on the spatial distribution of ground deformation in the past and in recent years are fundamental for adequately constraining deformation source models; therefore, we used many archaeological, topographical and geological constraints available in the existing scientific literature.

Geological setting

The Campi Flegrei is a ~ 12-km-sized active caldera with about one-third submerged (Pozzuoli Gulf; Fig. 1a). The current morphology resulted from several eruptions since 80 ka, with two main ignimbrite events producing the present-day shape of a nested caldera (e.g., Acocella 2008; Orsi et al. 2022 and references therein), namely the Campanian Ignimbrite (CI, dated at ~ 40 ka; Giaccio et al. 2017) and the Neapolitan Yellow Tuff (NYT, dated at ~ 15 ka; Deino et al. 2004). Since the last caldera-forming eruption, the volcanic activity focused within the caldera rims with over 70 events clustered in three main epochs of volcanic activity (Di Vito et al. 1999; Orsi et al. 2004; Isaia et al. 2015, 2021; Bevilacqua et al. 2015, 2016) accompanied by intense seismo-volcanic activity (Vitale et al. 2019; 2022). As a result, the nested caldera comprises distinct structural rims (Vitale and Isaia 2014; Fig. 1a). Recent studies of the caldera offshore (Natale et al. 2022b) highlighted the presence of three distinct caldera rims referred to as inner, medial and outer (Fig. 1a) associated with the CI eruption subsequently reactivated with the NYT eruption. In the western caldera sector, the inner rim is defined by several ~ N–S trending fault segments, including the Bacoli (Fig. 3a) and Baia faults. According to Natale et al. (2022b), the motion of the Bacoli Fault and, in general, of all the fault segments of the western inner caldera (Fig. 1a) is coupled with the dome resurgence, and were continuously active in the last 10 kyr with a total displacement, referred to the NYT top, of 30–50 m and a maximum displacement rate ranging between 3 and 5 mm/y. Furthermore, the Bacoli Fault shows the upper tip located ~ 100 m b.s.l.
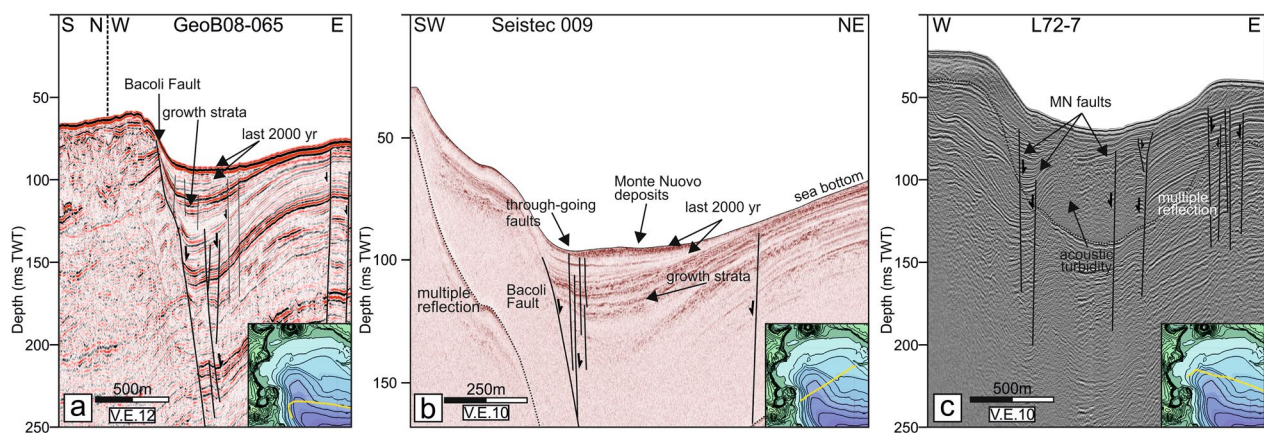
Fig. 3 **a** W–E-oriented seismic profile GeoB08-065, showing the Bacoli Fault and its synthetic faults accommodating the creep displacement along the western segment of the caldera inner-ring fault (modified after Natale et al. 2022a, b). **b** NE–SW-oriented high-resolution Seistec-009 shows the mainly plastic deformation of seismic units above the creeping Bacoli Fault and also cuts Monte Nuovo deposits (modified after Natale et al. 2020; 2022b). **c** WNW–ESE oriented seismic profile L72 shows the creeping Monte Nuovo Faults (modified after Aiello et al. 2012). *VE* vertical exaggeration. For locations, see the bottom-right inset

with the overlying strata diffusely deformed (sensu Hardy 2013; Fig. 3a, b).

Although no seismic lines cross the Baia Fault, this important structure shows morphological evidence of its activity in the topography and bathymetry. It crosses the Fondi di Baia volcano (Tarchini et al. 2019), down throwing the eastern part, whereas, to the north, it bounds the Punta Epitaffio tuff cliff (Fig. 1b), placing the old tuff rocks (14 ka, Bevilacqua et al. 2016) in structural contact with recent sediments. In addition, this fault is mapped in the official cartography (ISPRA 2022) as an eruptive fissure associated with the Baia–Fondi di Baia eruption sequence (dated at ~ 9.6 ka; Pistolesi et al. 2017). Furthermore, as evidenced by the increased thickness of marine sediments (La Starza Unit, Isaia et al. 2019; Vitale et al. 2019) in the Lucrino-Monte Nuovo area (Di Vito et al. 1999), the Baia Fault acted for a long-time at least since 10 ka, reactivating a segment of the inner ring faults (Natale et al. 2022a, b).

Another important fault system in the western sector is the Monte Nuovo Faults, associated with the 1538 CE eruption, spanning from a few hundred metres south of the current coast to the Monte Nuovo pyroclastic cone (Fig. 3c; Di Napoli et al. 2016). These faults are characterized by some normal faults likely related to dike-induced faulting (sensu Trippanera et al. 2015), as suggested by

the acoustic turbidity typical of dikes, such as observed in seismic profiles (Wall et al. 2010). However, in this area, like the Bacoli Fault, the Monte Nuovo Faults are blind structures with continuous deformation above the upper tip (Fig. 3c), a typical feature for such faults considering the low competence of the shallow infill of the Pozzuoli Gulf.

Archeological data

To restore the effects of the volcano-tectonic deformation on the topography, we tested five archaeological sites from Passaro et al. (2013) and a 1 m resolution Lidar-derived DEM (Digital Elevation Model) of the area, acquired in 2013 by Città Metropolitana di Napoli (http://sit.cittametropolitana.na.it/), down-sampled to 10 m resolution, stitched to the high-resolution bathymetry of the Pozzuoli Gulf (Somma et al. 2016) (Fig. 1a). Archeological data (Table 1) include the paved road of the Via *Herculanea* (sites 1 and 4), *Villa dei Pisoni* complex (sites 2 and 3) and the entry channel of the *Baianus Lacus* (site 5) (Fig. 4a). According to the archaeological reconstructions (Passaro et al. 2013) the paved road of the Via *Herculanea* and the breakwater system of the *Villa dei Pisoni* complex were built at 0.6 ± 0.1 m a.s.l. (i.e. functional elevation), whereas the inner court of the

Table 1 Archaeological data

Name	X	Y	Z	PFE	Structure	Age	References
1	423,343.2	4,519,981	− 6 ± 1	0.6 ± 0.1	Paved road of the Via Herculanea	100 BC	(Passaro et al. 2013)
2	422,311.9	4,519,303	− 5.9 ± 1	1 ± 0.1	Inner court of the Villa dei Pisoni complex	100 BC	(Passaro et al. 2013)
3	422,411.9	4,519,152	− 6.3 ± 1	0.6 ± 0.1	Breakwater system of the Villa dei Pisoni complex	100 BC	(Passaro et al. 2013)
4	422,488.2	4,519,476	− 6.6 ± 1	0.6 ± 0.1	Paved road of the Via Herculanea	100 BC	(Passaro et al. 2013)
5	422,188.1	4,519,031	− 6 ± 1	1 ± 0.1	Entry channel of the Baianus Lacus	100 BC	(Passaro et al. 2013)

Z actual depth (m below the actual sea level), *PFE* presumed functional elevation above the past mean sea level
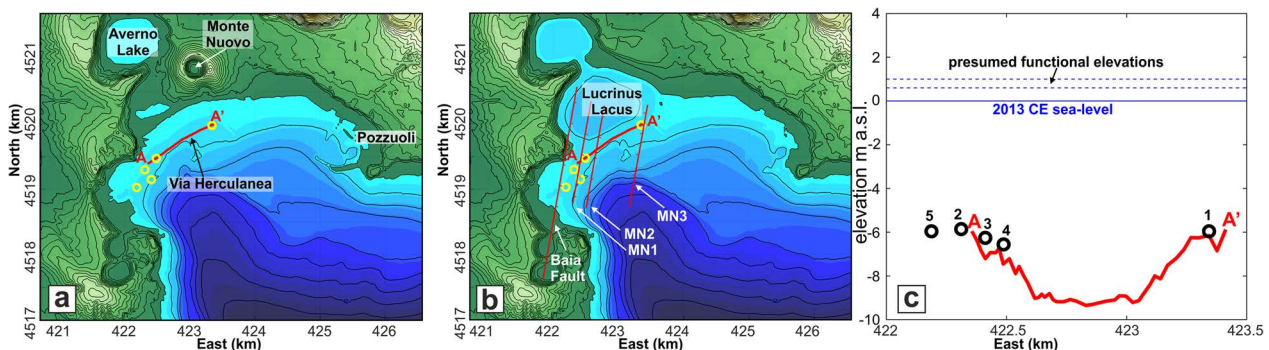

Fig. 4 **a** Topography and bathymetry of the Baia-Pozzuoli area in 2013. **b** Topography with the removal of the Monte Nuovo cone and products such as reconstructed by Di Vito et al. (1987) and Ascione et al. (2020). **c** Current elevations of the archaeological data and profile A–A′, the latter corresponding to the Via *Herculanea*

Villa dei Pisoni complex and the entry channel of the *Baianus Lacus* were built at 1 ± 0.1 m a.s.l.

Following Passaro et al. (2013), for all 2013 elevation data, we used an uncertainty of 1 m, selecting these archaeological data for their similar construction age of *ca.* 100 BCE. Furthermore, we used the topographic profile A–A' (Fig. 4a) corresponding to the trace of the Via *Herculanea* such as reconstructed by Passaro et al. (2013), Di Vito et al. (1987) and Ascione et al. (2020), whose age is about 100 BCE. Finally, we utilized a reconstructed topography with the removal of the Monte Nuovo cone and its products (Fig. 4b) in agreement with the available archaeological and paleo-morphological reconstructions (Di Vito et al. 1987; Ascione et al. 2020).

Topographic restoration

To investigate the volcano-tectonic causes of the drowning of the western sector of the Campi Flegrei caldera, we first evaluated the ground deformation effect related to the caldera inflation/deflation (bradyseism) phenomenon and, subsequently, the deformation associated with the fault activity that affected the area surrounding Baia.

Caldera inflation/deflation restoration

In the Campi Flegrei, the bradyseism phenomenon occurs as a ground deformation with a radial symmetry characterized by maximum uplift and subsidence vertical displacement values in the centre (Bevilacqua et al. 2020). Repeated levelling, GNSS, and InSAR measurements have focused on ground displacement (Amoruso et al. 2014; De Martino et al. 2021; Dvorak and Mastrolorenzo 1991; Iannaccone et al. 2018).

Figure 5a shows the normalized values of the vertical displacement (Amoruso et al. 2014; Dvorak and Mastrolorenzo 1991) obtained by (i) levelling measurements in different unrest periods both in uplift (1980–1983 and 1983–1984) and subsidence (1905/1907–1919,1985–1988 and 1989–1992); (ii) GPS measurements for the 21 stations in different periods within the 2000–2019 interval. Figure 5c also shows the horizontal displacement normalized to the maximum vertical displacement obtained by (i) EDM measurements in the period 1980–1983 (Amoruso et al. 2014 and references therein) and (ii) GPS data (2000–2019) (De Martino et al. 2021).

Normalized data with respect to the maximum vertical displacement indicate that the vertical and horizontal components of the ground show the same shape, independently of the time scale and the polarity of ground deformation (inflation or deflation). In particular, the normalized vertical displacement shows an axisymmetric bell shape (Fig. 5a) with a maximum in the centre and values approaching zero radially moving away from the centre. This pattern is due to robust control of the caldera

boundaries on the ground deformation; in fact, the recent ground uplift and subsidence are confined within a circle of ~6 km in diameter, corresponding to the caldera inner rim (De Natale et al. 1997; Bevilacqua et al. 2020; Fig. 1a).

According to several authors (Bevilacqua et al. 2020; De Martino et al. 2021; Iannaccone et al. 2018), the ongoing radial deformation centre is located in the Pozzuoli Gulf, with its surface projection located a few hundred metres south of the benchmark 25A/GPS RITE station (Fig. 1a). We used the point with UTM coordinates 426,200 m and 4,519,000 m as the deformation centre such as indicated by Iannaccone et al. (2018) (Fig. 4b). Finally, we used the vertical displacement recorded at the benchmark 25A/GPS RITE station as the value that reasonably approximates the maximum displacement to normalize both vertical and horizontal measurements.

The inflation/deflation ground deformation pattern at Campi Flegrei, during the unrest of the last decades and preceding the eruption of Monte Nuovo has been the subject of source modelling by several authors (Amoruso et al. 2014; Di Vito et al. 2016; Dvorak and Berrino 1991; Gottsmann et al. 2007; Macedonio et al. 2014).

However, fitting the available data to a specific inflation/deflation source model to restore the topography goes beyond the scope of this work. On the other hand, we estimated and applied the best-fit curves for both displacement components, with the recent normalized displacement pattern overlapping with that of the last 2100 yr (Amoruso et al. 2017; Di Vito et al. 2016). Similarly, this deformation pattern was remarkably comparable in the last 10 kyr, when the caldera floor experienced different cycles of inflation and deflation, resulting in the exposure of marine sediments of the La Starza Unit (Isaia et al. 2019; Natale et al. 2022a). Our reconstruction starts at 100 BCE, corresponding to the construction ages of most of the considered Roman archaeological sites and the Via *Herculanea* (Aucelli et al. 2020; Costa et al. 2022). Best-fit equations are shown in Fig. 5a, c. As discussed before, the normalized vertical deformation pattern (Fig. 5a, b) slopes down, moving away from the deformation centre. For example, for the *Serapis* Temple, the normalized vertical displacement is about 0.91 of the maximum uplift/subsidence; in contrast, the *Baianus Lacus* normalized vertical displacement ranges between 0.1 and 0.2. On the other hand, the normalized horizontal component pattern (Fig. 5c, d) shows a minimum in the centre, a maximum (0.4, normalized to the vertical deformation) in the annular area located 1.5–3 km from the centre, and declines to zero at a larger distance (>8 km).

To nullify the net ground subsidence between 100 BCE and 2013, we first calculated the elevation of the *Serapis* Temple at $t = 100$ BCE (Fig. 1b) and $t = 2013$ (Fig. 1c), assuming a linear subsidence trend between
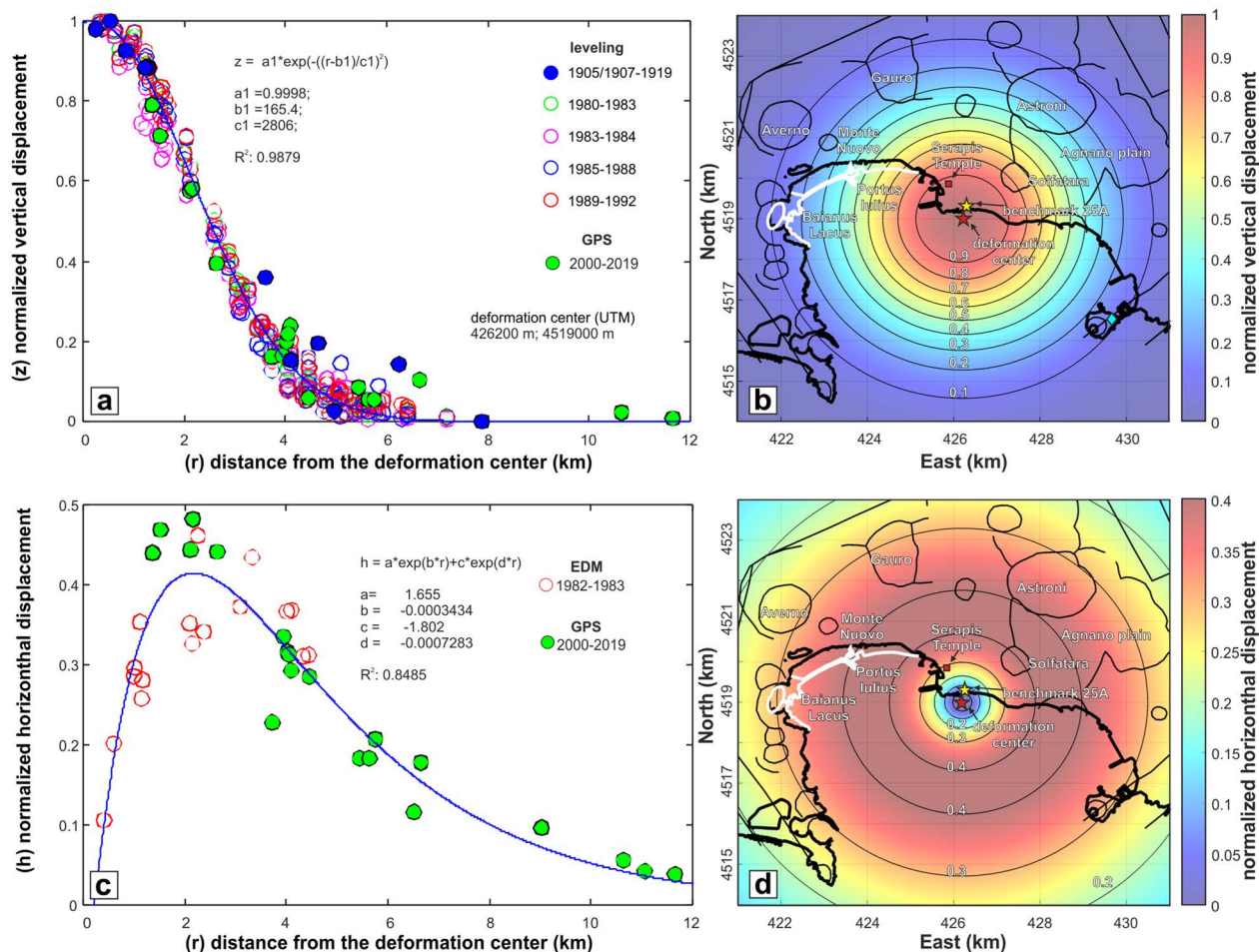
Fig. 5 a Normalized values of vertical displacement vs distance from the maximum deformation centre of levelling measurements during uplift and subsidence periods between 1905 and 1992 (data from Amoruso et al. 2014; Dvorak and Mastrolorenzo 1991), 2000–2019 GPS data (De Martino et al. 2021). **b** Contour plot of the best-fit curve of the normalized vertical displacement. **c** Normalized values of horizontal displacement vs distance from the maximum deformation centre of EDM measurements during 1982–1983 (data from Amoruso et al. 2014) and 2000–2019 GPS data (De Martino et al. 2021). **d** Contour plot of the best-fit curve of the normalized horizontal displacements

the measured points P1 and P2 of Fig. 1b (Bellucci et al. 2006; Morhange et al. 1999). The *Serapis* Temple was 6.2 m (above 2013 sea level) at 100 BCE and 0.25 m in 2013. Hence the net subsidence is 5.95 m in the interval 100 BCE-2013. To reconstruct the subsidence shape in this period, we estimated the maximum displacement as $Z_{max} = Z_{SerapisTemple}/0.91$, where the value 0.91 is the normalized displacement of the *Serapis* Temple (Fig. 4b). Subsequently, we removed such subsidence, deforming the DEM with net uplift associated with the dome deformation with $Z_{max} = 6.54$ m (100 BCE–2013 CE) with a conservative uncertainty of ± 2.5 m such as the measured point at 200 BCE (Fig. 1b). Finally, elevation data were corrected with the sea level at 100 BCE, as estimated by Lambeck et al. (2011) corresponding about to -1 m below the 2013 s.l. The sea level correction has been obtained by averaging the curves of sites 8 and 9

provided by Lambeck et al. (2011). The mean curve is expressed by the equation:

$S = -0.0039T6 + 0.174T5 - 2.8851T4 + 21.11T3 - 50.88T2 - 128.66\ T + 610.29$, where S is the sea level (expressed in metres), and T is the time before the present (expressed as kyr). The equation is valid in the time interval of 6-0 ka.

After restoring the contribution of caldera deflation alone (Fig. 6a), the resulting topography (with a z_{max} of 6.54 m) clearly shows that the *Baianus Lacus* area and most of the Via *Herculanea* and *Portus Iulius* would still have been submerged at 100 BCE. To estimate the quantitative effect of this restoration, we used as deformation markers the archaeological data (1–5) and profile A–A' (Fig. 6a, b). When restored, this area would still have been underwater with the *Via Herculanea* at a maximum depth of ~ 6.5 m b.s.l. in the central part. Even
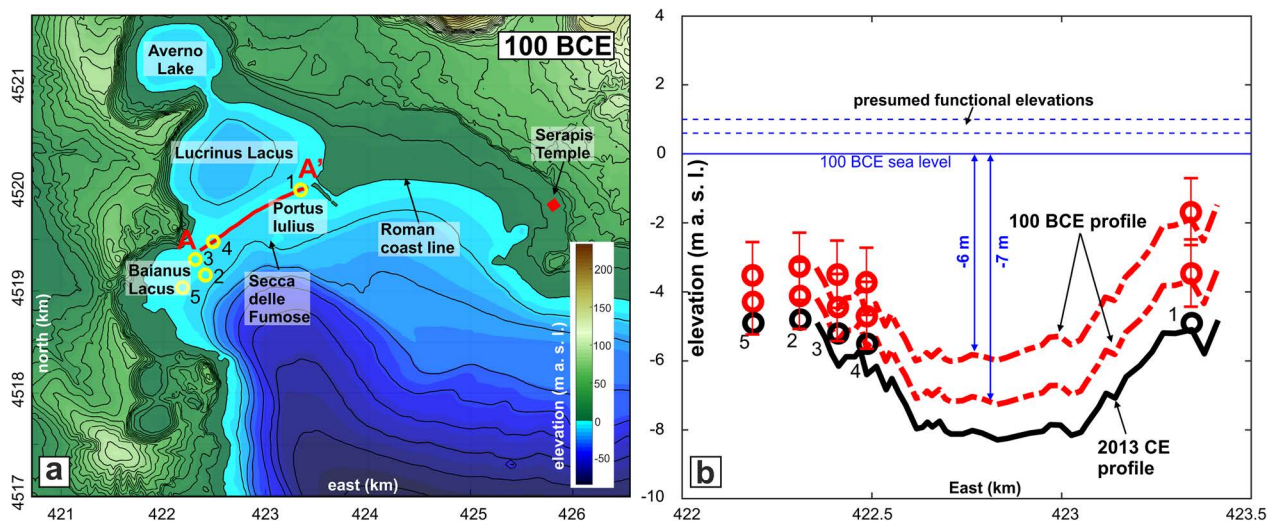
Fig. 6 **a** Topographic reconstruction following the dome (bradyseism) restoration at 100 BCE alone ($z_{max}=6.54$ m). **b** Restoration of archaeological data and A–A' topographic profile (the trace is shown in Fig. 5a) at 100 BCE; the black circles and curve are the 2013 archaeological sites and A–A' profile, whereas the red circles and curves are the restored elevations resulting from the maximum and minimum values of z_{max}

considering the upper boundary of the restoration, all data would still be below sea level (Fig. 6b).

Fault restoration

Different geophysical, geological, and morphological features suggest the activity of volcano-tectonic faults along the western side of the Campi Flegrei offshore in the last 2100 yr (e.g., Di Napoli et al. 2016; Natale et al. 2022a, b; Vitale and Isaia 2014). In the presented fault restoration, we considered the Baia and Monte Nuovo faults as a possible source of the drowning of the caldera western sector. To restore the ground deformation associated with these faults, we applied the Okada92 model (Okada 1992) by a Matlab© script (Battaglia et al. 2013). The Okada92 model furnishes solutions for displacements and tilts in 3D caused by a rectangular dislocation in a homogenous, isotropic, flat, and elastic half-space. We consider only the deformation of a free surface represented by the topographic (DEM) and bathymetric (DTM) surfaces. The model accounts for all dislocation types, including strike-slip, dip-slip, or tensile kinematics. The fault parameters are: (1) the position of the upper corner of the plane (xi, yi, xf, yf); (2) the upper and lower depth of the plane (zt, zb); (3) the dip (0–90°) and (4) the slip (m). At the same time, considering NYT and CI rocks as presentative of the substrate rocks, the Poisson's ratio v is 0.3, whereas the mean shear modulus m of 0.73 GPa (Heap et al. 2020). We applied reverse kinematics for each structure to restore the effect of normal faulting. The Matlab© script furnishes the vertical and horizontal (East and North components) displacements. In addition to the Baia Fault, we considered in the model

three faults representative of the deformation related to the Monte Nuovo eruption (MN1-3; Fig. 4b). We performed a Monte Carlo simulation by varying the slip values of the selected four faults, the dome deformation, and the position of the Monte Nuovo Faults to estimate the best deformation restoration. We assumed some geometric features of faults according to the geological and morphological evidence (all fault parameters are listed in Table 1). Firstly, we fixed the direction of all faults to N10E, in agreement with Di Napoli et al. (2016). Subsequently, we considered all structures as deep-seated blind normal faults with continuous deformation above the upper tip, as suggested by the seismic profiles of the area (Fig. 2; Aiello et al. 2012; Natale et al. 2020, 2022b). We considered the Baia Fault running from the Fondi di Baia up to the *Lucrinus Lacus* with a length of 3 km, whereas we adopted a length of 1.6 km for the Monte Nuovo Faults (MN1-3). The latter system comprises two faults dipping to the east (MN1, 2) and one dipping to the west (MN3), bounding a graben structure. We adopted for all faults a dip of 70°, as observed for most faults in the Pozzuoli Gulf (Natale et al. 2022b) and on-land (Vitale and Isaia 2014). Finally, we selected an uncertainty of the Monte Nuovo Faults location of ± 100 m on the East component, a slip range of 0–15 m for all faults to run the iterations. The dome deformation varies between 4 and 9 m according to the uncertainty (± 2.5 m) affecting the elevation of the *Serapis* Temple in 100 BCE (Fig. 1c). Slip and dome deformation values were generated by the Matlab© function Random with a uniform distribution. We filtered Monte Carlo simulations by selecting only the solutions well-fitting with the original topography,

considering that at least 70% of the archaeological data and profile points corresponding to the Via *Herculanea* fall within the interval 0–2 m above the 100 BCE sea level. The simulation provided 100,000 topographic profiles and archaeological site elevations (Fig. 7a), of which ~ 2200 were considered suitable. The fault features for the Monte Carlo simulation are displayed in Table 2, including the resulting mean slip values with the uncertainties.

While the fault slip frequencies (Fig. 7b) show a bell-like distribution, the dome deformation frequency diagram is almost flat (Fig. 7b). We selected some slip values within the interval of the slip ranges provided by the Monte Carlo simulation to reconstruct a likely 100 BCE topography (Fig. 7c) and the restoration of the archaeological data and A–A′ profile (Fig. 7d). In this reconstruction, the *Baianus Lacus* and *Portus Iulius* would have entirely emerged, and *Secca delle Fumose* would be an islet such as reported by the historical sources (Aucelli et al. 2020 and references therein). The reconstructed profile A–A′ (Fig. 7d) shows that the elevation of Via *Herculanea* is between 0 and 2 m above the 100 BCE sea level. A profile that accounts only for the Baia Fault and dome restoration is also provided (green line in Fig. 7d); finally, Fig. 7e shows the restoration of the *Serapis* Temple site. According to the reconstruction of Fig. 1b, the elevation of the *Serapis* Temple floor was 6.2 m above the current s.l. and 7.3 m above the 100 BCE s.l., whereas, in 2013, it was 0.25 m above the current s.l. and 1.35 m above the 100 BCE s.l. After the complete restoration, it would be ~ 7.7 m above the 100 BCE s.l.

Discussion

The presented work proposes a novel interpretation of the causes of the drowning of the Roman villas of *Baiae* and the western side of the harbour of *Portus Iulius*. This study illustrates how the severe subsidence that affected the western sector of the Campi Flegrei in the last 2100 yr was related to the volcano-tectonic activity mainly expressed by the normal faults located across the Campi Flegrei caldera western inner ring. Unlike the widely accepted opinion that the caldera deflation (bradyseism) is responsible for the subsidence in the western sector of the caldera, we demonstrate that the vertical ground movement associated with this phenomenon only marginally affected this sector. The effect of the dome restoration on the elevation of archaeological data and topographic A–A′ profile is secondary, being in the order of 10–20% of the maximum displacement (z_{max}) near the inner ring faults (Fig. 5b). This feature is confirmed by the flat frequency diagram of dome height (Fig. 7b) resulting from the Monte Carlo simulation, highlighting the marginal role of the caldera deflation

in driving the subsidence of this sector, regardless of its magnitude (ranging between 4 and 9 m).

On the contrary, in our view, the drowning was mainly caused by the long-lived activity of the Baia Fault that lowered, concurrently with the other inner rim faults such as the Bacoli Fault (Natale et al. 2022a, b), a large part of the Campi Flegrei western sector, and by the formation of a structural graben depression associated with the dike that fed the Monte Nuovo eruption. It must be emphasized that the proposed topographic reconstruction is based on a fault geometry with solid geological evidence, as previously illustrated (see paragraph 4.2); however, it represents only a possible scenario of the effects of the volcano-tectonic history that characterizes this area. In the presented model, we used three faults for the ground subsidence associated with the Monte Nuovo eruption. However, this is a minimum number of faults; in fact, the model furnishes reasonable solutions, also increasing the number of structures with smaller displacements. The choice of characteristics of the faults (i.e. strike, dip, and kinematics) used in the model has been constrained by robust geological evidence. In fact, the formation of a depression bounded by normal faults is consistent with the ground deformation on the top of a magmatic dike (e.g., Magee and Jackson 2021), such as hypothesized for the Monte Nuovo eruption (e.g., Di Vito et al. 2016). Furthermore, the strike and dip of the selected faults are well-defined by the geological evidence reported in the available literature (Vitale and Isaia 2014; Di Napoli et al. 2016; Natale et al. 2022b). Hence, in our simulations, we have only varied the relatively poorly constrained fault features, i.e. the amount of displacement and the exact location of the faults.

Generally, the selected archaeological elevation interval, when restored considering the activity of the Baia and Monte Nuovo faults and the effect of the bradyseism, falls within the presumed functional elevation range (i.e. the elevation at the time they were operational; Fig. 7d), as indicated by Passaro et al. (2013; Table 1). In addition, the restoration of the *Serapis* Temple (Fig. 7e) indicates that the restored elevation (7.7 m above the 100 BCE s.l.) is within the uncertainty of the 7.3 m value estimated by the curve of Fig. 1b (Bellucci et al. 2006; Morhange et al. 1999).

The Monte Carlo simulation also indicates that the mean slip of the Baia Fault is 6.8 ± 3.4 m in the last 2100 yr. Assuming that, as some other ring faults of the western inner caldera (Natale et al. 2022b), this structure always acted, the mean displacement rate is 3.2 ± 1.6 mm/y, estimated for a temporal interval of 2100 years. This displacement rate range is comparable to that calculated for the Bacoli Fault. However, the mean slip value is higher than the surficial subsidence
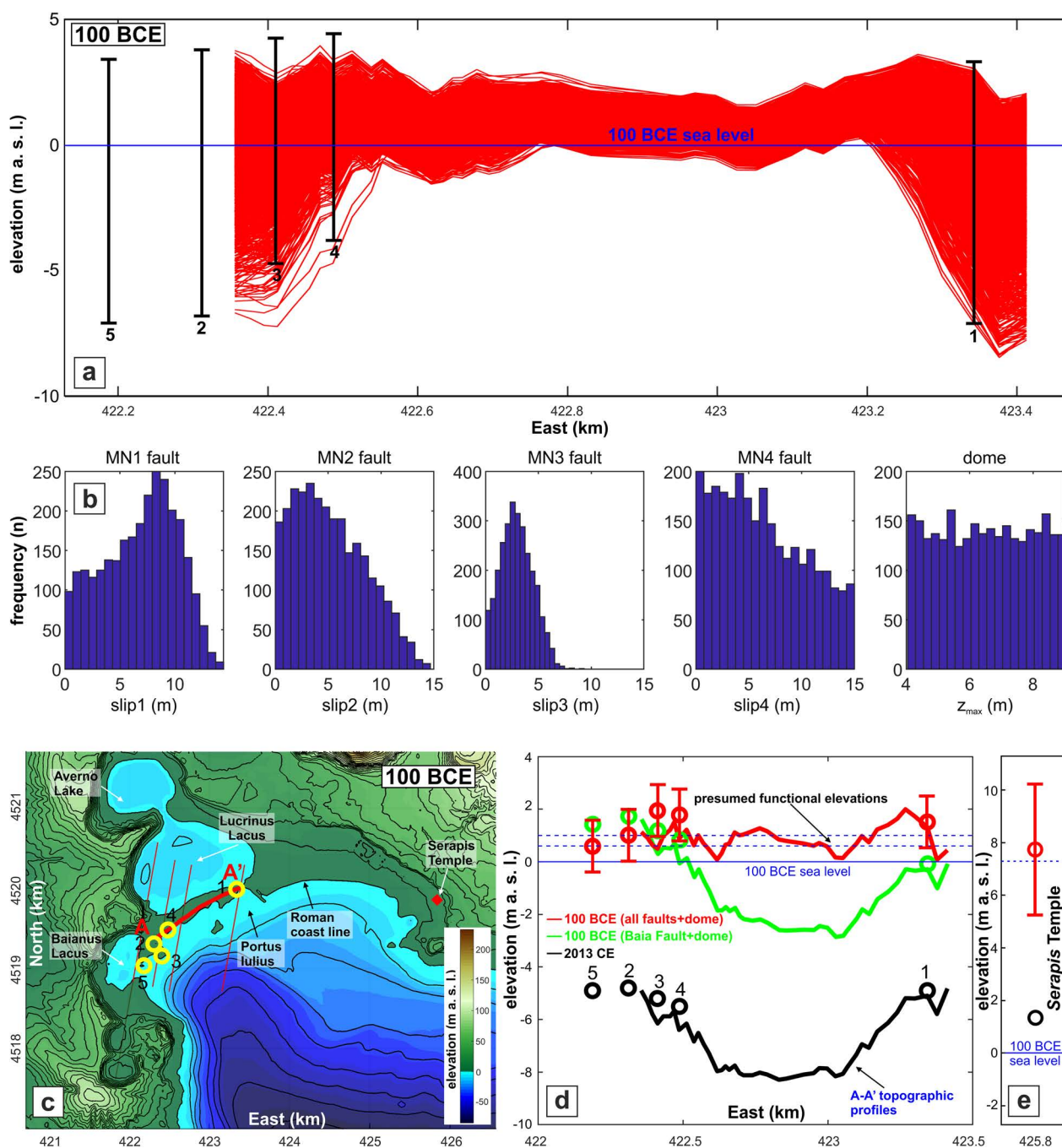
Fig. 7 Monte Carlo simulation: **a** restoration of archaeological data (1–5) and A–A' profile (Via *Herculanea*); **b** frequency histograms of the fault slips (in metres) and dome deformation (z_{max} in metres). **c** 2D topographic reconstruction after restoring the ground deformation associated with all faults and dome activity with mean values resulting from the Monte Carlo simulation. **d** Elevation of the archaeological sites (red circles) and A–A' profile (red curve) using the mean values resulting from the Monte Carlo simulation. The diagram also shows the 2013 elevations (black circles and curve) and the 100 BCE elevations (green circles and curve), considering only the Baia Fault and dome restoration. **e** Elevations of the *Serapis* Temple: in 2013 (black circle) and in 100 BCE (red circle)

rate of 2.9 ± 0.5 mm/y estimated by archaeological features (Fig. 7d) and Passaro et al. (2013). This dissimilarity might be the consequence of (i) the effect of the

graben formation associated with the Monte Nuovo Faults, which produced an uplift of the footwalls (including the Baia sector) and (ii) the decrease of the Baia Fault

Table 2 Okada92 model fault parameters and results of the Monte Carlo simulation

Fault name	Type	xi (m)	yi (m)	xf (m)	yf (m)	zt (m b.s.l.)	zb (m b.s.l.)	Dip (°)	Slip (m)	Mean slip (m)	St. dev (m)	Selected slip (m)
Baia	'dip'	421,834	4,517,620	422,361	4,520,570	100	3000	70	0–15	**6.8**	**3.4**	**9.7**
MN1	'dip'	422,366 ± 100	4,518,770	422,595 ± 100	4,520,350	100	3000	70	0–15	**5.2**	**3.3**	**2.6**
MN2	'dip'	422,496 ± 100	4,518,710	422,775 ± 100	4,520,290	100	3000	70	0–15	**2.9**	**1.5**	**3.3**
MN3	'dip'	423,154 ± 100	4,518,710	423,435 ± 100	4,520,290	100	3000	70	0–15	**6.3**	**4.1**	**2.9**

slip upward where the displacement is expressed as continuous deformation above the tip such as modelled by Okada92 model.

It is worth noting as the Via *Herculanea* currently is submerged up to a maximum of ~8 m b.s.l. (Fig. 6b), and *Baianus Lacus* of ~4 m b.s.l. By restoring the deformation of the Baia Fault and dome deformation only (Fig. 7d, green profile), the Via *Herculanea* would be again underwater at a maximum of ~3 m b.s.l. It follows that the drowning of the central sector of the *Portus Iulius* was mainly related to the activity of the Monte Nuovo Faults, as suggested by Passaro et al. (2013), who related the collapse of the Via *Herculanea* to the Monte Nuovo fracture system. The strong subsidence peak of other geoarchaeological markers of different ages in the same area supports our reconstruction (Marino et al. 2022 and references therein), suggesting active volcano-tectonic processes along the western ring fault (Natale et al. 2022b).

The proposed model, which combines the caldera inflation/deflation deformation with the faults' motion, adequately reproduces the ground deformation evolution of the Baia-*Portus Iulius* area; however, this is a simplified model, and further, more in-depth structural studies may furnish more information to better constrain the paleo-topographic reconstructions. Furthermore, for the sake of clarity, the observed subsidence in the western side of the caldera might also be explained by more complex models involving, for example, magmatic multi-source or arbitrarily oriented and shaped sources; however, the proposed model provides, to date a new and more geologically constrained explanation of the peculiar geodetic pattern and archaeological evidence in this area of the Campi Flegrei, opening new scenarios on the interpretation of the submersion of these Roman facilities.

In this paper, we highlight that the motion of volcano-tectonic faults within the Campi Flegrei caldera can overprint the bell-shaped deformation pattern, and we cannot exclude that also other sectors of the caldera and/or surrounding areas may be affected by similar processes, and may require further studies. However, it must be marked as the two volcano-tectonic processes (faulting and doming) may record different displacement values at different time scales. For example, the inner ring faults show displacement of about 3 mm/yr in the last 2100 yr, whereas the Monte Nuovo Faults reasonably have much higher displacement rates since they are associated with the short-lived eruption of the Monte Nuovo volcano (Guidoboni and Ciuccarelli 2011). On the other hand, the bradyseism may show a spectrum of vertical displacement rate values, ranging from a few mm/yr during the subsidence stages such as occurred in geological (Isaia et al. 2019), historical (Di Vito et al. 2016) and monitoring times (Dvorak and Berrino 1991), up to a few m/yr during the uplift phases such as occurred before the Monte Nuovo eruption (Di Vito et al. 2016) or in the 1982–1984 unrest (e.g., Orsi et al. 1999).

In the western sector of the caldera, reports of historical seismicity felt by the population, possibly of moderate magnitude, have been reported mainly before and after the Monte Nuovo eruption (Guidoboni and Ciuccarelli 2011; Rovida et al. 2020), and we cannot exclude that the Baia Fault and, more probably, the Monte Nuovo Faults have triggered earthquakes during that late-unrest stage. On the other hand, seismic activity is not expected during the subsidence stages, such as evidenced in the well-monitored 1985–2005 period (e.g., D'Auria et al. 2011), where seismicity, focused only in the Solfatara volcano area, occurred in the so-called mini-uplifts (Gaeta et al. 2003). However, in analogy with the Bacoli Fault, characterized by a lack of stick–slip faulting, and by continuous deformation, also evidenced by growth strata in the hanging wall (Fig. 3a), we retain that the Baia Fault may not have produced significant earthquakes in the last 2100 yr.

In Fig. 8, we present the reconstructed topography at 100 BCE, displaying the landscape during the Roman urbanization of the area. According to the historical reconstructions, the presented topographic restoration shows the Baia area, including a coastal lake and the coastal sector in front of the current Punta Epitaffio, where luxury villas were built, and a littoral sand spit joining the *Baiae* with the *Puteoli* areas, shielding the *Lucrinus Lacus*.
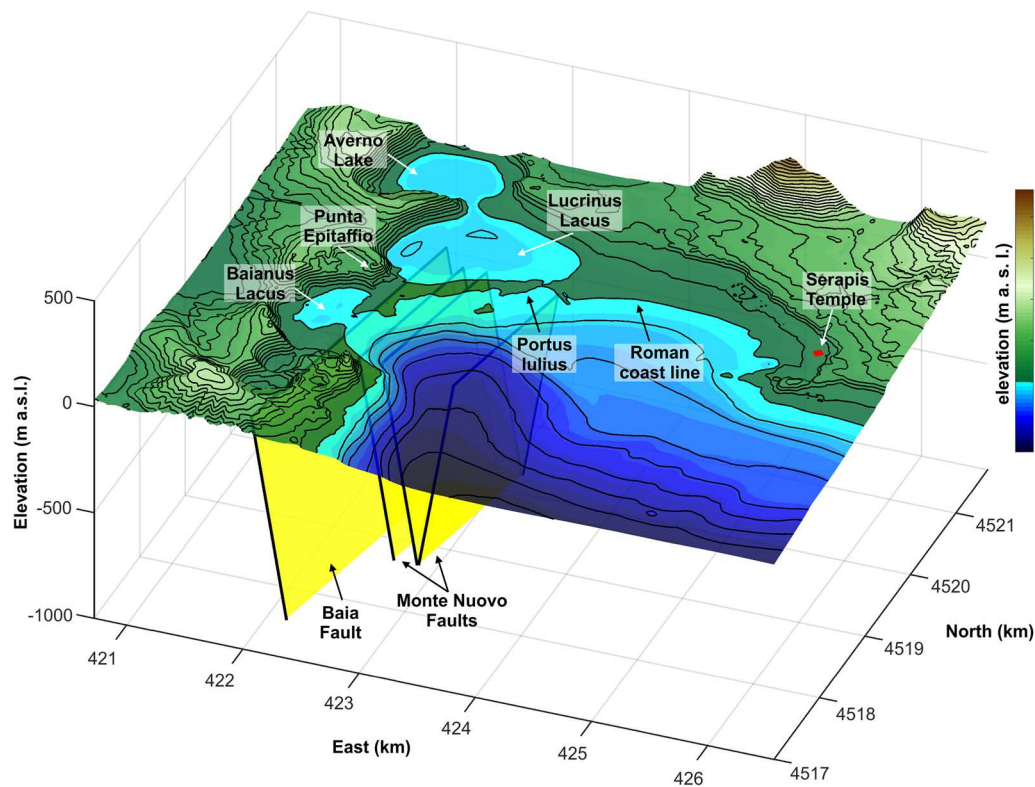
Fig. 8. 3D view of the reconstructed topography and bathymetry at 100 BCE showing the Baia and Monte Nuovo faults

Finally, it is interesting to note as there is another example of a Roman harbour presently submerged. It is the case of Sinuessa, a Roman city located in the northern sector of the Campania Plain, 42 km to the north of Campi Flegrei. Although it is in a different tectonic context, it experienced a similar subsidence of ∼ 6.5 m in the last 2300 yr (Pennetta et al. 2017), and such as the model proposed in this work, the causes may be sought in the activity of normal faults (Pennetta et al. 2017).

In sum, this study attempted to shed light on the interaction between the activity of caldera ring faults and the intra-caldera inflation and deflation processes relying on several archaeological features available in the area. We proposed a novel interpretation for the ground deformation of a portion of the caldera by considering different deformation models with respect to a simplistic model accounting only for the bradyseism phenomenon, regardless of its source. This approach may also be applied to other active calderas worldwide characterized by complex volcano-tectonic settings and evolutions such as the Campi Flegrei caldera.

Concluding remarks

- We propose a volcano-tectonic model showing that ground inflation/deflation processes (bradyseism) alone cannot explain the drowning of Roman structures, and its role is marginal, especially for the westernmost sector.
- The proposed interpretation illustrates that the drowning of the western sector of the Campi Flegrei caldera, including the Roman luxury villas of *Baiae* and the *Portus Iulius*, is the result of the combined action of the caldera floor deflation and volcano-tectonic faulting.
- The subsidence since 200 BCE was mainly caused by the activity of the long-lived Baia Fault and further enhanced by the subsequent faulting developed during the 1538 CE eruption of Monte Nuovo.
- Archaeological data, together with the reconstructed Via *Herculanea* topographic profile, all with an age of *ca.* 100 BCE, were used to constrain a reconstruction that accounts for the ground deformation related to the bradyseism and volcano-tectonic faulting.

- We used the Okada92 model to estimate the ground deformation associated with faulting and a bell-shaped model fitted on levelling and GNSS data for the caldera inflation/deflation phenomenon.
- Restored archaeological and topographic data indicate that they fall within the interval of presumed functional heights, with a restored topography and bathymetry of the western sector of the Campi Flegrei caldera defined by the landscape showing the Baia area, where luxury villas were built, including the lake of *Baianus Lacus*, and the *Portus Iulius* formed by a littoral sand spit shielding the *Lucrinus Lacus* as represented by the historical reconstructions.
- This study marks the necessity to apply different ground deformation models to untangle the complex volcano-tectonic evolution that characterizes active volcanic fields worldwide, such as the Campi Flegrei caldera.

Abbreviations

BCE	Before Common Era
CE	Common Era
DEM	Digital elevation model
DTM	Digital terrain model
GNSS	Global Navigation Satellite System
EDM	Electronic distance measurements
InSAR	Interferometric Synthetic Aperture Radar
m a.s.l.	Metres above sea level
MN	Monte Nuovo

Author contributions
S.V. and J.N. conceived the idea that faulting may drive subsidence in this caldera sector. S.V. performed the reconstruction at 100 BCE topography by restoring the ground deformation related to doming and faulting. S.V. created a Matlab© script to deform the DEM/DTM and perform the Monte Carlo simulation. J.N. contributed to the definition of the volcano-tectonic framework. S.V. wrote the first draft of the paper. S.V. and J.N. edited and revised the manuscript. All authors read and approved the final manuscript.

Availability of data and materials
The datasets generated during and analysed during the current study are publicly available on OSF HOME at https://osf.io/f8e7j/?view_only=a262d3021cfe433d9ddfff74bb9b4d78.

Code availability
Topographic data were transformed using scripts developed by Matlab© version R2021a. Okada92 model was performed by Matlab© script (dMODELS) available from https://pubs.usgs.gov/tm/13/b1. The final figure layouts were prepared using CorelDraw Graphic Suite.

Declarations

Ethics approval and consent to participate
Not applicable.

Consent for publication
Not applicable.

Competing interests
There are no financial and non-financial competing interests for this work.

Author details
[1]Dipartimento di Scienze della Terra, dell'Ambiente e delle Risorse (DiSTAR), Università degli Studi di Napoli Federico II, Naples, Italy.

References

Acocella V (2008) Activating and reactivating pairs of nested collapses during caldera-forming eruptions: Campi Flegrei (Italy). Geophys Res Lett. https://doi.org/10.1029/2008GL035078

Acocella V (2019) Bridging the gap from caldera unrest to resurgence. Front Earth Sci 7:173

Aiello G, Marsella E, Di Fiore V (2012) New seismo-stratigraphic and marine magnetic data of the Gulf of Pozzuoli (Naples Bay, Tyrrhenian Sea, Italy): inferences for the tectonic and magmatic events of the Phlegrean Fields volcanic complex (Campania). Mar Geophys Res 33:97–125

Amoruso A, Crescentini L, Sabbetta I (2014) Paired deformation sources of the Campi Flegrei caldera (Italy) required by recent (1980–2010) deformation history. J Geophys Res: Solid Earth 119:858–879

Amoruso A, Crescentini L, D'Antonio M, Acocella V (2017) Thermally-assisted magma emplacement explains restless calderas. Sci Rep 7(1):1–9

Ascione A, Aucelli PPC, Cinque A, Di Paola G, Mattei G, Ruello M, Russo Ermolli E (2020) Geomorphology of Naples and the Campi Flegrei: human and natural landscapes in a restless land. J Maps 17:18–28

Aucelli PP, Brancaccio L, Cinque A (2017) Vesuvius and Campi Flegrei: volcanic history, landforms and impact on settlements. In Landscapes and landforms of Italy, Springer, pp 389–398

Aucelli PP, Mattei G, Caporizzo C, Cinque A, Troisi S, Peluso F, Stefanile M, Pappone G (2020) Ancient coastal changes due to ground movements and human interventions in the Roman Portus Julius (Pozzuoli Gulf, Italy): results from photogrammetric and direct 295 surveys. Water 12:658

Battaglia M, Troise C, Obrizzo F, Pingue F, De Natale G (2006) Evidence for fluid migration as the source of deformation at Campi Flegrei caldera (Italy). Geophys Res Lett 33:L01307

Battaglia M, Cervelli PF, Murray JR (2013) Modeling crustal deformation near active faults and volcanic centers—a catalog of deformation models. US geological survey techniques and methods 13, chap. B1, 96 p. https://pubs.usgs.gov/tm/13/b1

Bellucci F, Woo J, Kilburn CRJ, Rolandi G (2006) Mechanisms of activity and unrest at large calderas. Geol Soc Lond, Special Publications. 269:141–158

Berrino G, Corrado G, Luongo G, Toro B (1984) Ground deformation and gravity changes accompanying the Pozzuoli uplift. Bull Volcanol 47:187–200

Bevilacqua A, Isaia R, Neri A, Vitale S, Aspinall WP, Bisson M, Flandoli F, Baxter PJ, Bertagnini A, Esposti Ongaro T, Iannuzzi E, Pistolesi M, Rosi M (2015) Quantifying volcanic hazard at Campi Flegrei caldera (Italy) with uncertainty assessment: I. Vent opening maps. J Geophys Res Solid Earth 120:2309–2329

Bevilacqua A, Flandoli F, Neri A, Isaia R, Vitale S (2016) Temporal models for the episodic volcanism of Campi Flegrei caldera (Italy) with uncertainty quantification. J Geophys Res: Solid Earth 121:7821–7845

Bevilacqua A, Neri A, De Martino P, Isaia R, Novellino A, Tramparulo FDA, Vitale S (2020) Radial interpolation of GPS and leveling data of ground deformation in a resurgent caldera: application to Campi Flegrei (Italy). J Geodesy 94:24. https://doi.org/10.1007/s00190-020-01355-x

Costa A, Di Vito MA, Ricciardi GP, Smith VC, Talamo P (2022) The long and intertwined record of humans and the Campi Flegrei volcano (Italy). Bull Volcanol. https://doi.org/10.1007/s00445-021-01503-x

D'Auria L, Giudicepietro F, Aquino I, Borriello G, Del Gaudio C, Lo Bascio D, Martini M, Ricciardi GP, Ricciolinop P, Ricco C (2011) Repeated fluid-transfer episodes as a mechanism for the recent dynamics of Campi Flegrei caldera (1989–2010). J Geophys Res Solid Earth 116(B4)

D'Auria L, Pepe S, Castaldo R, Giudicepietro F, Macedonio G, Ricciolino P, Tizzani P, Casu F, Lanari R, Manzo M, Martini M, Sansosti E, Zinno I (2015) Magma injection beneath the urban area of Naples: a new mechanism for the 2012–2013 volcanic unrest at Campi Flegrei caldera. Sci Rep 5(1):1–11

De Martino P, Dolce M, Brandi G, Scarpato G, Tammaro U (2021) The Ground Deformation History of the Neapolitan Volcanic Area (Campi Flegrei Caldera, Somma-Vesuvius Volcano, and Ischia Island) from 20 years of continuous GPS observations (2000–2019). Rem Sens 13:2725

De Natale G, Petrazzuoli SM, Pingue F (1997) The effect of collapse structures on ground deformations in calderas. Geophys Res Lett 24(13):1555–1558

De Natale G, Troise C, Pingue F, Mastrolorenzo G, Pappalardo L, Battaglia M, Boschi E (2006) The Campi Flegrei caldera: unrest mechanisms and hazards. Geol Soc Lond, Special Publications. https://doi.org/10.1144/GSL.SP.2006.269.01.03

De Siena L, Chiodini G, Vilardo G, Del Pezzo E, Castellano M (2017) Source and dynamics of a volcanic caldera unrest: Campi Flegrei, 1983–84. Sci Rep 7:1–13

Deino AL, Orsi G, de Vita S, Piochi M (2004) The age of the Neapolitan Yellow Tuff caldera-forming eruption (Campi Flegrei caldera – Italy) assessed by $^{40}Ar/^{39}Ar$ dating method. J Volcanol Geoth Res 133:157–170

Del Gaudio C, Aquino I, Ricciardi GP, Ricco C, Scandone R (2010) Unrest episodes at Campi Flegrei: a reconstruction of vertical ground movements during 1905–2009. J Volcanol Geoth Res 195:48–56

Di Napoli R, Aiuppa A, Sulli A, Caliro S, Chiodini G, Acocella V, Ciraolo G, Di Vito MA, Interbartolo F, Nasello C, Valenza M (2016) Hydrothermal fluid venting in the offshore sector of Campi Flegrei caldera: a geochemical, geophysical, and volcanological study. Geochem Geophys Geosyst 17:4153–4178

Di Vito M, Lirer L, Mastrolorenzo G, Rolandi G (1987) The 1538 Monte Nuovo eruption (Campi Flegrei, Italy). Bull Volcanol 49:608–661

Di Vito MA, Isaia R, Orsi G, Southon J, De Vita S, D'Antonio M, Pappalardo L, Piochi M (1999) Volcanism and deformation since 12000 years at the Campi Flegrei caldera (Italy). J Volcanol Geoth Res 91:221–246

Di Vito MA, Acocella V, Aiello G, Barra D, Battaglia M, Carandente A, Del Gaudio C, de Vita S, Riccardi GP, Ricco C, Scandone R, Terrasi F (2016) Magma transfer at Campi Flegrei caldera (Italy) before the 1538 AD eruption. Sci Rep 6(1):1–9

Dvorak JJ, Berrino G (1991) Recent ground movement and seismic activity in Campi Flegrei, southern Italy: episodic growth of a resurgent dome. J Geophys Res: Solid Earth 96(B2):2309–2323

Dvorak JJ, Mastrolorenzo G (1991) The mechanism of recent vertical crustal movements in Campi Flegrei caldera, Southern Italy. Geology Society of America, Special Paper 263

Gaeta FS, Peluso F, Arienzo I, Castagnolo D, De Natale G, Milano G, Albanese C, Mita DG (2003) A physical appraisal of a new aspect of bradyseism: the miniuplifts. J Geophys Res 108(B8):2363. https://doi.org/10.1029/2002JB001913

Giaccio B, Hajdas I, Isaia R, Deino A, Nomade S (2017) High-precision 14C and 40Ar/39Ar dating of the Campanian Ignimbrite (Y-5) reconciles the timescales of climatic-cultural processes at 40 ka. Sci Rep 7:45940

Gottsmann J, Carniel R, Coppo N, Wooller L, Hautmann S, Rymer H (2007) Oscillations in hydrothermal systems as a source of periodic unrest at caldera volcanoes: multiparameter insights from Nisyros, Greece. Geophys Res Lett 34:L07307. https://doi.org/10.1029/2007GL029594

Guidoboni E, Ciuccarelli C (2011) The Campi Flegrei caldera: historical revision and new data on seismic crises, bradyseisms, the Monte Nuovo eruption and ensuing earthquakes (twelfth century 1582 AD). Bull Volcanol 73(6):655–677

Hardy S (2013) Propagation of blind normal faults to the surface in basaltic sequences: insights from 2D discrete element modelling. Mar Pet Geol 48:149–159

Heap MJ, Villeneuve M, Albino F, Farquharson JI, Brothelande E, Amelung F, Got J, Baud P (2020) Towards more realistic values of elastic moduli for volcano modelling. J Volcanol Geoth Res 390:106684

Iannaccone G, Guardato S, Donnarumma GP, De Martino P, Dolce M, Macedonio G, Chierici F, Beranzoli L (2018) Measurement of seafloor deformation in the marine sector of the Campi Flegrei caldera (Italy). J Geophys Res: Solid Earth 123:66–83

Isaia R, Vitale S, Di Giuseppe MG, Iannuzzi E, Tramparulo FDA, Troiano A (2015) Stratigraphy, structure and volcano-tectonic evolution of Solfatara maar-diatreme (Campi Flegrei, Italy). Geol Soc Am Bull 127:1485–1504

Isaia R, Vitale S, Marturano A, Aiello G, Barra D, Ciarcia S, Iannuzzi E, Tramparulo FDA (2019) High-resolution geological investigations to reconstruct the long-term ground movements in the last 15 kyr at Campi Flegrei caldera (southern Italy). J Volcanol Geother Res 385:143–158. https://doi.org/10.1016/j.jvolgeores.2019.07.012

Isaia R, Di Giuseppe MG, Natale J, Troiano A, Tramparulo FDA, Vitale S (2021) Volcano-tectonic setting of the Pisciarelli Fumarole Field, Campi Flegrei caldera, southern Italy: insights into fluid circulation patterns and hazard scenarios. Tectonics 40:e2020TC006227. https://doi.org/10.1029/2020TC006227

ISPRA (2022) https://www.isprambiente.gov.it/Media/carg/447_NAPOLI/Foglio.html

Lambeck K, Antonioli F, Anzidei M, Ferranti L, Leoni G, Scicchitano G, Silenzi S (2011) Sea level change along the Italian coast during the Holocene and projections for the future. Quatern Int 232(1–2):250–257. https://doi.org/10.1016/j.quaint.2010.04.026

Lima A, De Vivo B, Spera FJ, Bodnar RJ, Milia A, Nunziata C, Belkin HE, Cannatelli C (2009) Thermodynamic model for uplift and deflation episodes (Bradyseism) associated with magmatic hydrothermal activity at the Campi Flegrei active volcanic center (Italy). Earth Sci Rev 97:44–58

Lyell CG (1830–1833) Principles of geology: being an inquiry how far the former changes of the earth's surface are referable to causes now in operation; in 4 Volumes, Vol. 1. Murray, London.

Macedonio G, Giudicepietro F, D'Auria L, Martini M (2014) Sill intrusion as a source mechanism of unrest at volcanic calderas. J Geophys Res Solid Earth 119:3986–4000

Magee C, Jackson CAL (2021) Can we relate the surface expression of dike-induced normal faults to subsurface dike geometry? Geology 49(4):366–371

Marino C, Ferranti L, Natale J, Anzidei M, Benin A, Sacchi M (2022) Quantitative reconstruction of Holocene ground displacements in the offshore part of the Campi Flegrei caldera (southern Italy): perspectives from seismo-stratigraphic and archaeological data. Mar Geol 447:106797

Morhange C, Bourcier M, Laborel J, Giallanella C, Goiran JP, Crimaco L, Vecchi L (1999) New data on historical relative sea level movements in Pozzuoli, Phlaegrean Fields, southern Italy. Phys Chem Earth Part A 24:349–354

Morhange C, Marriner N, Laborel J, Todesco M, Oberlin C (2006) Rapid sea-level movements and noneruptive crustal deformations in the Phlegrean Fields caldera, Italy. Geology 34:93–96

Natale J, Ferranti L, Marino C, Sacchi M (2020) Resurgent dome faults in the offshore of the Campi Flegrei caldera (Pozzuoli Bay, Campania): preliminary results from high-resolution seismic reflection profiles. Bull Geophys Oceanogr 61(3):333–342

Natale J, Ferranti L, Isaia R, Marino C, Sacchi M, Spiess V, Steinmann L, Vitale S (2022a) Integrated on-land-offshore stratigraphy of the Campi Flegrei caldera: new insights into the volcano-tectonic evolution in the last 15 kyr. Basin Res 34(2):855–882. https://doi.org/10.1111/bre.12643

Natale J, Camanni G, Ferranti L, Isaia R, Sacchi M, Spiess V, Steinmann L, Vitale S (2022b) Fault systems in the offshore sector of the Campi Flegrei caldera (southern Italy): implications for nested caldera structure, resurgent dome, and volcano-tectonic evolution. J Struct Geol 163:104723. https://doi.org/10.1016/j.jsg.2022.104723

Okada Y (1992) Internal deformation due to shear and tensile faults in a half-space. Bull Seismol Soc Am 82:1018–1040

Orsi G, Civetta L, Del Gaudio C, De Vita S, Di Vito MA, Isaia R, Petrazzuoli SM, Ricciardi GP, Ricco C (1999) Short-term ground deformations and seismicity in the resurgent Campi Flegrei caldera (Italy): an example of active block-resurgence in a densely populated area. J Volcanol Geoth Res 91(2–4):415–451

Orsi G, Di Vito MA, Isaia R (2004) Volcanic hazard assessment at the restless Campi Flegrei caldera. Bull Volcanol 66:514–530

Orsi G, D'Antonio M, Civetta L (eds.) (2022) Campi Flegrei. Active volcanoes of the world, Springer, Berlin, Heidelberg, pp 201–217

Parascandola A (1947) I fenomeni bradisismici del Serapeo di Pozzuoli. Stabilmento tipografico G. Genovese

Passaro S, Barra M, Saggiomo R, Di Giacomo S, Leotta A, Uhlen H, Mazzola S (2013) Multi-resolution morpho-bathymetric survey results at the Pozzuoli-Baia underwater archaeological site (Naples, Italy). J Archaeol Sci 40(2):1268–1278

Pennetta M, Stanislao C, Donadio C (2017) Sulle possibili cause della sommersione dell'approdo di epoca romana di Sinuessa, in Pennetta, M., Trocciola, A. "Sinuessa, un approdo sommerso di epoca romana—archeologia, geomorfologia costiera, strategie sostenibili di valorizzazione". ENEA, ISBN: 978-88-8286-340-1

Pistolesi M, Bertagnini A, Di Roberto A, Isaia R, Vona A, Cioni R, Giordano G (2017) The Baia-Fondi di Baia eruption at Campi Flegrei: stratigraphy and dynamics of a multi-stage caldera reactivation event. Bull Volcanol 79(9):1–18. https://doi.org/10.1007/s00445-017-1149-1

Rispoli C, De Bonis A, Esposito R, Graziano SF, Langella A, Mercurio M, Morra V, Cappelletti P (2020) Unveiling the secrets of Roman craftsmanship: mortars from Piscina Mirabilis (Campi Flegrei, Italy). Archaeol Anthropol Sci. https://doi.org/10.1007/s12520-019-00964-8

Rovida A, Locati M, Camassi R, Lolli B, Gasperini P (2020) The Italian earthquake catalogue CPTI15. Bull Earthq Eng 18(7):2953–2984

Somma R, Iuliano S, Matano F, Molisso F, Passaro S, Sacchi M, Troise C, De Natale G (2016) High-resolution morpho-bathymetry of Pozzuoli Bay, southern Italy. J Maps 12:222–230

Tarchini L, Ranaldi M, Carapezza ML, Di Giuseppe MG, Isaia R, Lucchetti C, Prinzi EP, Tramparulo FDA, Trioano A, Vitale S (2019) Multidisciplinary studies of diffuse soil CO_2 flux, gas permeability, self-potential, soil temperature highlight the structural architecture of Fondi di Baia craters (Campi Flegrei caldera, Italy). Ann Geophys 62(1):1–12. https://doi.org/10.4401/ag-7683

Todesco M, Neri A, Esposti Ongaro T, Papale P, Rosi M (2006) Pyroclastic flow dynamics and hazard in a caldera setting: application to Phlegrean Fields (Italy). Geochem Geophys Geosyst 7:Q11003

Todesco M, Costa A, Comasytri A, Colleoni F, Spad G, Quareni F (2014) Vertical ground displacement at Campi Flegrei (Italy) in the fifth century: rapid subsidence driven by pore pressure drop. Geophys Res Lett 41:1471–1478. https://doi.org/10.1029/2013GL059083

Trippanera D, Ruch J, Acocella V, Rivalta E (2015) Experiments of dike-induced deformation: insights on the long-term evolution of divergent plate boundaries. J Geophys Res: Solid Earth 120(10):6913–6942

Vaselli O, Tassi F, Tedesco D, Poreda JR, Caprai A (2011) Submarine and inland gas discharges from the Campi Flegrei (southern Italy) and Pozzuoli Bay: geochemical clues for a common hydrothermal-magmatic source. Proc Earth Planet Sci 4:57–73

Vitale S, Isaia R (2014) Fractures and faults in volcanic rocks (Campi Flegrei, Southern Italy): insight into volcano-tectonic processes. Int J Earth Sci 103:801–819

Vitale S, Isaia R, Ciarcia S, Di Giuseppe MG, Iannuzzi E, Prinzi EP, Tramparulo FDA, Troiano A (2019) Seismically induced soft-sediment deformation phenomena during the volcano-tectonic activity of Campi Flegrei caldera (southern Italy) in the last 15 kyr. Tectonics 38:1999–2018. https://doi.org/10.1029/2018TC005267

Vitale S, Natale J, Isaia R, Tramparulo FDA, Ciarcia S (2022) Evidence of seismic-related liquefaction processes within the volcanic record of the Campi Flegrei caldera (Italy). Geosciences 12(6):241

Wall M, Cartwright J, Davies R, McGrandle A (2010) 3D seismic imaging of a Tertiary Dyke Swarm in the Southern North Sea, UK. Basin Res 22(2):181–194

Woo JYL, Kilburn CRJ (2010) Intrusion and deformation at Campi Flegrei, southern Italy: sills, dikes, and regional extension. J Geophys Res 115:B12210

Publisher's Note